Published in final edited form as:

Brain Struct Funct. 2017 August ; 222(6): 2819–2830. doi:10.1007/s00429-017-1374-6.

Prefrontal-hippocampal coupling by theta rhythm and by 2–5 Hz oscillation in the delta band: The role of the nucleus reuniens of the thalamus

Alexis Roy[*], **Frans Pettersson Svensson**[*], **Amna Mazeh**, and **Bernat Kocsis**

Harvard Medical School, Department of Psychiatry, Beth Israel Deaconess Medical Center

Abstract

Rhythmic synchronization of hippocampus (HC) and prefrontal cortex (PFC) at theta frequencies (4–8 Hz) are thought to mediate key cognitive functions and disruptions of HC-PFC coupling was implicated in psychiatric diseases. Theta coupling is thought to represent a HC-to-PFC drive transmitted via the well-described unidirectional HC projection to PFC. In comparison, communication in the PFC-to-HC direction is less understood, partly because no known direct anatomical connection exists. Two recent findings, i.e. reciprocal projections between the thalamic nucleus reuniens (nRE) with both PFC and HC and a unique 2–5 Hz rhythm reported in the PFC, indicate however that a second low-frequency oscillation may provide a synchronizing signal from PFC to HC via nRE. Thus in this study we recorded local field potentials in the PFC, HC, and nRE to investigate the role of nRE in PFC-HC coupling established by the two low-frequency oscillations. Using urethane-anesthetized rats and stimulation of pontine reticular formation to experimentally control the parameters of both forebrain rhythms, we found that theta and 2–5 Hz rhythm were dominant in HC and PFC, respectively, but were present and correlated in all three signals. Removal of nRE influence, either statistically (by partialization of PFC-HC correlation when controlling for the nRE signal) or pharmacologically (by lidocaine microinjection in nRE), resulted in decreased coherence between the PFC and HC 2–5-Hz oscillations, but had minimal effect on theta coupling. This study proposes a novel thalamo-cortical network by which PFC-to-HC coupling occurs via a 2–5 Hz oscillation and is mediated through the nRe.

Keywords

Slow rhythms; Synchronization; 4 Hz oscillation; Thalamo-cortical network; Midline thalamus; Cortico-hippocampal coupling

Introduction

Oscillatory synchronization at low frequencies (<15 Hz) is a powerful mechanism by which neural networks coordinate their activities. Slow oscillations are transmitted with minor phase delay between distant brain regions, and thus provide a flexible signal to synchronize neuronal firing and locally generated fast (high beta, gamma) oscillations in these structures

Correspondence: Bernat Kocsis MD PhD, bkocsis@hms.harvard.edu, 617-735-3301.

[*]AR and FPS contributed equally this research

(Buzsaki 2002). In particular, rhythmic synchronization of hippocampus (HC) and prefrontal cortex (PFC) are thought to mediate key cognitive functions, such as working memory (Benchenane et al. 2010; Sauseng et al. 2010; Anderson et al. 2010; Hyman et al. 2005) or goal-directed spatial navigation (Ito et al. 2015). Disruptions in HC-PFC coupling may mediate some of the pathophysiology of schizophrenia (Cousijn et al. 2015; Dickerson et al. 2010; Sigurdsson et al. 2010; Vertes 1981). The overwhelming majority of prior studies emphasized the role of PFC-HC coupling at theta frequency (Anderson et al. 2010; Benchenane et al. 2010; O'Neill et al. 2013; Sauseng et al. 2010; Siapas et al. 2005; Jones and Wilson 2005; Hyman et al. 2005). Theta rhythm is the most prominent oscillatory signal in the rodent brain generated by the septo-hippocampal network (Buzsaki 2002; Vertes and Kocsis 1997), and thus theta coupling tacitly assumes driving by the HC. Since however PFC is thought to play a key role integrating cognitive function, a functional network should also exist to allow the PFC to communicate back to the HC and other structures to modify behavior (Miller and Cohen 2001). It was indeed proposed recently that HC-PFC coupling also involves a second rhythm of PFC origin that co-occurs with HC theta and can mediate driving by PFC (Fujisawa and Buzsaki 2011). The frequency of this oscillation varies between 2–5 Hz in the upper delta range but its regularity, with sharp spectral peak, clearly distinguishes this signal from wide-band (1–4 Hz) delta activity mostly recorded in sleep.

Regular 2 Hz oscillations in PFC also occur in rats anesthetized with urethane (Kiss et al. 2011a; Kiss et al. 2011d). In this preparation, theta rhythm has been routinely recorded in HC, where it spontaneously alternates with wide-band delta (large irregular activity, (Kramis et al. 1975)) or is elicited by electrical stimulation of the pontine reticular formation (RPO) (Vertes 1981; McNaughton and Sedgwick 1978; Li et al. 2007; Ly et al. 2013). The dominant frequency of spontaneous theta under urethane anesthesia is around 4 Hz, but tail pinch or RPO stimulation shift the frequency up, across the entire theta range (4–10 Hz). RPO-elicited theta under urethane involves both atropine-sensitive and atropine-resistant mechanisms (Li et al. 2007), and the linear correlation between RPO stimulus intensity and theta frequency and amplitude provides an experimental model to study neuronal mechanisms and to use as biomarker in drug discovery (McNaughton et al. 2007). PFC 2 Hz rhythm was not studied in this experimental paradigm and thus the first goal of this study was to test whether RPO stimulation can modify the slow PFC rhythm as well as HC theta, and whether there is any meaningful relationship between the two signals. As we expected, RPO stimulation shifted the frequency of PFC oscillations in a stimulus intensity-dependent manner within the entire “awake” range of 2–5 Hz. The amplitude of this signal however decreased with increasing stimulus intensity, i.e. changed in the direction opposite to HC theta.

The second goal of this study was to examine how this PFC oscillation is communicated to HC in this model. Abundant anatomical and electrophysiological evidence demonstrate the existence of a direct unidirectional HC-to-PFC pathway (Ferino et al. 1987; Swanson 1981; Thierry et al. 2000; Jay and Witter 1991; Hoover and Vertes 2007) mediating HC theta drive to PFC (Anderson et al. 2010; Benchenane et al. 2010; O'Neill et al. 2013; Sauseng et al. 2010; Siapas et al. 2005; Jones and Wilson 2005; Hyman et al. 2005). In comparison, communication in the PFC-to-HC direction is less understood, partly because no known direct anatomical connection exists. Recent tracing studies demonstrate however that PFC

fibers form synaptic connections with the thalamic nucleus reuniens (nRE) neurons that then project to the HC (Herkenham 1978; Vertes et al. 2007). Thus, the nRE may provide the critical anatomical link between the PFC and HC (Vertes et al. 2015). Thus, we hypothesized that nRE plays a specific role in 2–5 Hz PFC-to-HC synchronization, whereas theta coupling may use the direct HC-to-PFC projection. In this study, we recorded local field potential oscillations in the PFC, HC, and nRE in the urethane-anesthetized rat, while stimulating RPO, and demonstrated that removal of nRE influence, either statistically (using partial correlations) or experimentally (by pharmacologic inactivation), resulted in decreased coherence between the PFC and hippocampal 2–5-Hz oscillations, but had minimal effect on theta coupling.

Methods

Animals

15 male Sprague-Dawley rats (300–550 g, Charles River Laboratories in Massachusetts) were used in this study. The procedures described were conducted in accordance with the Institutional Animal Care and Use Committee of Harvard Medical School and Beth Israel Deaconess Medical Center.

Surgical procedures and electrophysiological recordings

All animals were anesthetized using urethane (1.2–1.5 g/kg of 65–80% solution, intraperitoneal injections). Urethane anesthesia allows for spontaneous theta oscillations in the HC through stimulation of the pontine reticular formation (Kramis et al. 1975; Vertes 1981; Vertes and Kocsis 1997). The animals' head were fastened in a stereotaxic frame, and small burred wholes were made to allow for electrode placement. Two pairs of twisted stainless steel wires with 1mm distal separation were implanted in HC (3.7 mm posterior to bregma, 2.2 mm lateral to midline, and 4.8 mm below the brain surface), and nRE (2.5 mm posterior to bregma, on the midline, and 6.5 mm below the brain surface). Two single electrode wires were implanted in the right and left PFC (3.2 mm anterior to bregma, 0.5 mm lateral to midline, and 4.8 mm below the brain surface). A pair of stimulating stainless steel electrodes was implanted in the reticular nucleus pontis oralis (RPO) (8 mm posterior to bregma, 1.5 mm lateral to midline, and 8 mm below the brain surface). Skull screws overlying the nasal bone and cerebellum served as the reference and ground electrode, respectively. Electrode wires and screws were secured with dental cement. Hippocampal theta rhythm was elicited by electrical stimulation of the RPO (0.1 ms square waves at 100 Hz for a duration of 10 s separated by >60 s). Five stimulation intensities were used, evenly distributed between two thresholds empirically identified in each individual rat, at the beginning of the experiment (Li et al. 2007; Ly et al. 2013). The first threshold marked the minimum intensity that produces hippocampal theta rhythm and the second corresponded to the maximal intensity after which theta frequency or amplitude did not change. To identify the exact values of stimulation currents to elicit this standard response, covering the entire range of theta frequencies, at the beginning of experiment a series of various stimulation intensities (range 0.1 mA-1mA) were applied until the thresholds were found. Once the correct range was obtained, five levels of stimulus intensity were applied in random order.

Pharmacological inactivation of the thalamic nucleus reuniens

In 4 rats, a guided cannula was implanted in the nRE along with pairs of recording electrodes in the PFC (one in each side), and the right dorsal (dHC) and ventral hippocampus (vHC) and stimulating electrodes in the RPO. After control recording, lidocaine (0.2 mg/microliter, volume of 1 microliter) was microinfused using a syringe pump at a rate of 347 nanoliters/min. Theta was elicited through RPO stimulation and electrophysiological recordings were performed as described.

Histological procedure

After experiment completion, the rats were deeply anesthetized, and brains were removed and fixed in formalin. The brains were sectioned at 50 microns in the coronal plane using a freezing microtome. Sections were stained with the Nissl method, and slides were examined to confirm electrode placement. The locations of PFC electrodes were verified in the prelimbic cortex, HC electrodes in above and below the HC fissure, and nRE electrodes in the midline, in or in the close vicinity of nRE.

Data Analysis

Local field potentials of the HC, PFC, and nRE during 10 s RPO stimulation were extracted. The middle six seconds of the stimulus was selected, and filtered between 1 and 70 Hz and sampled at 256 Hz. Signals were subjected to Fast Fourier Transform, and power density spectra were obtained. Frequencies with greatest power (peak frequencies) were identified in the HC and PFC, respectively. In the HC, these frequencies corresponded to theta oscillations; the peak power values were then calculated for the PFC and nRE signals for this previously identified theta oscillation. In the PFC, these frequencies corresponded to the 2–5 Hz oscillations in the delta frequency range; the peak power was then calculated for the HC and nRE signal at this previously identified 2–5 Hz oscillation. Spectra were normalized across experiments whereas the minimum and maximum of the peak power at any of the two frequencies across all stimulation instances for a given electrode in a given experiment was calculated and power values were then corrected by subtracting the minimum and dividing by the range to obtain values between 0 and 1. Linear regression analysis was applied to peak frequencies (theta and 2–5 Hz) versus stimulus intensity. Linear regression analysis was also applied to peak power in the PFC, HC, and nRE vs. stimulus intensity for the theta and 2–5 Hz signals. Pearson's correlation was calculated between the peak power values of the HC and PFC for both the theta and 2–5 Hz oscillations. Partial correlations were also calculated between peak power of the HC and PFC with controlling for the nRE signal, using the following formula:

$$\mathrm{r}\left(\frac{\mathrm{PFC}-\mathrm{HC}}{\mathrm{nRe}}\right)=\frac{r\left(\mathrm{PFC}-\mathrm{HC}\right)-r\left(\mathrm{PFC}-\mathrm{nRe}\right)*r\left(\mathrm{HC}-\mathrm{nRe}\right)}{\sqrt{\left(1-r(\mathrm{PFC}-\mathrm{nRe})^{2}\right)*\left(1-r(\mathrm{HC}-\mathrm{nRe})^{2}\right)}}$$

For rats that underwent lidocaine inhibition of the nRE, coherence spectra between the HC and PFC local field potentials were calculated for all pairwise combinations between 2 PFC (left and right prelimbic area) and 4 HC (2 in dHC, 2 in vHC, on the right side) signals

during RPO stimulations repeated before and after local nRE administration of lidocaine. Coherence was calculated on overlapping 4 s windows resulting in coherence spectra with 0.5 Hz resolution. Peak coherence values were identified in the delta and theta ranges at RPO stimulus intensities optimal for these oscillations, i.e. at low intensities for delta and at high intensities for theta oscillations generating the largest peaks in the power spectra (see Results).

Results are reported as mean ± standard error of the mean, unless specified otherwise.

Results

As described previously (Vertes and Kocsis 1997), HC activity in urethane anesthetized rats spontaneously alternated between two states characterized by large amplitude irregular activity and theta rhythm (Fig. 1A–C). PFC also showed this pattern of similar irregular activity alternating with a dominant rhythm that appeared however at lower frequencies (~ 2 Hz) in the delta band (Kiss et al. 2011a; Kiss et al. 2011d), co-occurring with HC theta. Frequently, a strong oscillatory component also appeared mixed within the background of irregular delta activity in the “passive” state (see e.g. sharp spectral peak on top of wide-band delta in Fig. 1D). Furthermore, this rhythm was also present, along with theta, in LFP recordings in the nRE as well as in HC (Fig. 1E).

Both the appearance of LFP traces and the spectral representation of the rhythmic PFC signal showed essential similarities with HC theta rhythm and was drastically different from wide-band delta activity, limited on one side (~0.5 Hz) by the high-pass filter of AC coupled recording and on the other side (~4 Hz) slowly tapering toward higher frequencies of the delta band. Thus, to avoid confusion of these fundamentally different delta-band activities we use the term “2–5 Hz oscillations” to denote sinusoidal-like delta activity, dominating the PFC signal in “active” states. The two types of delta activity occur in un-anesthetized animals, in different behavioral states. Wide-band delta activity is well known as the dominant EEG pattern of slow wave sleep whereas highly synchronized neuronal firing generating sinusoidal LFP in PFC was reported in awake rats during working memory task, referred to as “4 Hz oscillation” (Fujisawa and Buzsaki 2011).

RPO stimulation induces 2–5 Hz oscillation in PFC, simultaneously with HC theta rhythm

Electrical stimulation of the RPO resulted in reliable sinusoidal oscillations in the PFC, HC, and nRE. Two prominent rhythms were observed which were generally present in all three signals to different degrees, depending on the intensity of RPO stimulation. Figure 2 shows an example in which at low intensity (0.15 mA; Fig 2B), 2–5 Hz oscillation dominated the PFC signal, theta dominated the HC signal (at 2.7 and 6.3 Hz, respectively), and both rhythms were present in the nRE (Fig. 2F). Increasing the stimulus intensity (0.33 mA; Fig. 2C) changed this pattern to synchronized theta oscillations (at 7.6 Hz) in all three locations (Fig. 2D–F). The frequency and power of both oscillations systematically changed as the RPO stimulations varied (Fig. 3A–C). As in previous studies (Li et al. 2007; Ly et al. 2013), the peak frequency of theta rhythm was between 5.4 Hz ± 0.26 and 7.4 Hz ± 0.24 and

increased linearly with increasing stimulus intensity (r = 0.64, p <0.001). The frequency of PFC 2–5 Hz oscillation varied between 2.7 Hz ± 0.19 and 3.7 Hz ± 0.3 (range: 1.9 – 5.1 Hz) and also increased linearly with increasing stimulus intensity (r = 0.37, p = 0.001) (Fig. 3D).

For each stimulation episode, peak theta frequencies were identified in the HC, and peak spectral power at these frequencies was obtained for all three signals and normalized across experiments (see Methods). Peak theta power increased linearly in the HC (r = 0.63, p <0.001) with increasing stimulus intensity. There was little effect of stimulus intensity on spectral power at theta frequency in the PFC (r = 0.11, p= 0.36) or nRE (r = 0.06, p = 0.59), i.e. on average, peak power of theta elicited by RPO stimulation did not change significantly as stimulus intensity increased. However, in individual experiments PFC and nRE theta often showed increasing trends and specifically, in a subset of animals (n=7) with strong HC-PFC relationship (see below), PFC theta, although weak, did show significant increase with stimulus intensity (r=0.36, p=0.03) (Fig. 3E, dashed line)".

Peak frequencies of the 2–5 Hz oscillation were identified in the PFC, and spectral power at these frequencies was obtained for the PFC, HC, and nRE for each stimulation episode. Contrary to the behavior of theta rhythm, PFC 2–5 Hz peak power decreased linearly with increasing stimulus intensity (r = −0.60, p <0.001). Peak 2–5 Hz power was similar in the nRE (r = −0.60, p <0.001). It was consistently lower in HC but showed a similar negative trend as RPO stimulation changed (r = −0.36, p = 0.001) (Fig. 3F). Taken together, these results demonstrated that theta oscillation power in the HC increased with greater RPO stimulation, whereas the 2–5 Hz oscillations followed the opposite trend by decreasing PFC, HC, and nRE power with increasing RPO stimulation, suggesting a possible negative relationship between the generation of the two rhythms.

Differential contribution of nRE to PFC-HC 2–5 Hz and theta coupling

Although 2–5 Hz and theta oscillations were most prominent in the PFC and HC, respectively, they were also observed in the two other structures, including the nRE, where they followed similar RPO stimulation-dependent variations in their frequency and power (Fig. 3). To test the possibility of the common origin of each, i.e. PFC for 2–5 Hz and HC for theta rhythm, we next calculated pairwise correlations between peak oscillatory power in different areas. The first analysis included all stimulation episodes (>450 in 15 rats; Fig. 4A–B) and showed significant (p < 0.001) relationship between each LFP pair, at both frequencies, correlations for 2–5 Hz being consistently stronger than for theta (Fig. 4C). The largest correlation was found between PFC and nRE (r = 0.82), about 30% larger than for the two other pairs (r = 0.5 for both PFC-HC and HC-nRE). Similarly, the strongest theta correlation was between nRE and the presumed origin of theta rhythm (p = 0.37 for HC-nRE vs. p = 0.2 for the other two LFP signal pairs) (Fig. 4C).

We then tested correlations in individual experiments for each pair at both 2–5 Hz and theta frequencies, shown in Fig. 4D. When calculated separately in each rat in this second analysis (Fig. 4D–F), significant correlations were found at 2–5 Hz in the majority experiments (87–93%; i.e. in 14 rats between PFC-nRE and in 13 rats for the other 2 pairs; Fig. 4D, blue). On the other hand, theta correlations between PFC and HC were only significant in 7 out of 15

(47%) rats, whereas theta was significant in 11 rats (73%) between HC and nRE and in 9 rats (60%) between nRE and PFC (Fig. 4D, red). Group averages indicated a similar structure of correlations (Fig. 4E–F), i.e. 2–5 Hz larger than theta, and the largest correlations for either 2–5 Hz or theta between nRE and the presumed origin of these oscillations.

The strong correlation between nRE at the two rhythms with the structures of their presumed origin, especially remarkable for PFC-nRE (Fig. 4B), suggested that nRE may serve as a relay to establish PFC-HC oscillatory coupling. nRE is reciprocally connected to both PFC and HC which allows for the three structures to synchronize their activities. Thus in the third analysis, we used partial correlation to calculate the residual PFC-HC correlation after allowance was made for the variations in the rhythmic components of the nRE signal. Only significant correlations were partialized, i.e. for this analysis we only used the experiments in which PFC-HC correlations were significant at both 2–5 Hz and theta frequencies (n=7; Fig. 5A–B, note larger PFC-HC and smaller HC-nRE correlations in this group). For 2–5-Hz oscillations we found a significant decrease in PFC-HC correlation when controlling for nRE (student's paired t-test, $p < 0.001$), from $r = 0.81 \pm 0.03$ to $r = 0.13 \pm 0.12$ (Fig. 5C–E) indicating that nRE contributes to 2–5-Hz synchrony between the PFC-HC, and removal of this influence completely eliminates residual PFC-HC correlation. In contrast, theta PFC-HC correlations ($r = 0.65 \pm 0.07$) and partial correlation ($r = 0.61 \pm 0.08$) were not significantly different (students paired t-test, $p = 0.53$), suggesting that nRE has minimal effect on theta synchronization between PFC and HC (Fig. 5C–E). Interestingly, HC-nRE theta correlation was lower in this group ($p = 0.32$, Fig. 5A–B), which was then completely eliminated when controlling for the PFC (partial correlation r(HC-nRE/PFC) = 0.007) indicating that no unique HC-nRE theta coupling existed in these experiments other than that also shared with PFC (Fig. 5E).

A similar analysis performed on the group of experiments with significant PFC-HC correlation at 2–5 Hz (n=13) showed the same result ($r = 0.74 \pm 0.05$ and $r = 0.01 \pm 0.1$, before and after partialization for 2–5 Hz). Partial correlation analysis on the entire population (n=15, using original correlation values without zeroing non-significant correlations) also consistently showed elimination of PFC-HC 2–5 Hz correlation when controlling for nRE ($r = 0.68 \pm 0.06$ to $r = 0.006 \pm 0.1$), but no effect on theta correlation theta ($r = 0.38 \pm 0.09$ and $r = 0.40 \pm 0.1$), or on any other combination of signals for either 2–5 Hz or theta correlation.

The effect of nRE inhibition on PFC-HC coupling

Lidocaine was microinfused into the nRE to pharmacologically inhibit its potential contribution to PFC-HC oscillatory coupling. In these experiments, HC field potentials were recorded both in dHC and vHC (2 electrodes in each site), which allowed comparisons based on a total of 8 pairwise combinations of PFC-HC recordings in each rat. Peak coherence values were identified in the delta and theta ranges at RPO stimulus intensities optimal to generate the largest spectral peaks of the two oscillations and compared before and after local lidocaine administration (Fig. 6A, note shift in theta peak frequency from 7.2 ± 0.1 to 5.9 ± 0.2, $p=0.02$). Lidocaine had little effect on coherence for the theta oscillation

(coherence pre-lidocaine = 0.52 ± 0.04, post-lidocaine = 0.48 ± 0.04, p = 0.19, n=32) although it decreased peak theta frequency (7.2 ± 0.1 to 5.9 ± 0.2, p=0.02), suggesting that the nRE does not participate in propagation of theta oscillations between HC and PFC. In contrast, PFC-HC coherence of 2–5 Hz oscillation significantly decreased after lidocaine by 0.39 ± 0.04 (Fig. 6C) from 0.73 ± 0.03 control to 0.34 ± 0.04 after lidocaine (Fig. 6D; $p < 0.001$, n=32). The effect was similar in dHC and vHC (Fig. 6B). These results support the hypothesis that PFC-to-HC delta synchrony is at least partly mediated by the nRE, as pharmacologic inactivation of this nucleus significantly decreases coherence between these two brain regions.

Discussion

The major findings of this study are that (1) HC-PFC coupling can be established not only by HC theta rhythm but also by a second narrow-band oscillations in the 2–5 Hz range dominating PFC activity and that (2) the thalamic nRE is essential for PFC-HC coupling by this second rhythm whereas theta drive may use the direct HC-PFC pathway.

HC theta and HPC 2–5 Hz (~4 Hz) oscillations in bidirectional HC-HPC coordination

Our study was performed in rats under urethane anesthesia using RPO stimulation—a commonly used model that allows experimental control over forebrain oscillations without behavioral confines (McNaughton et al. 2007)—and showed that the same experimental paradigm can be applied to investigate HC theta and PFC slow oscillations. Importantly, the appearance of field potential traces and the spectral representation of the rhythmic PFC signal showed essential similarities with HC theta rhythm, and were drastically different from wide-band delta activity. Furthermore, RPO stimulation intensity effectively controlled the frequency and amplitude of both oscillations. Just as the frequency of spontaneous theta rhythm which appears at the lower end (~4 Hz) of the theta band can be increased up to 7–8 Hz by RPO stimulation (Li et al. 2007; Ly et al. 2013; McNaughton and Sedgwick 1978), the frequency of the 2–5 Hz PFC oscillation which spontaneously occurs at ~2 Hz (Kiss et al., 2011a, 2011b) can be increased by RPO stimulation to generate sharp spectral peaks across the entire 2–5 Hz range found in awake rats (Fujisawa and Buzsaki 2011). We also found that, as in the awake animal, both theta and this 2–5 Hz oscillation were commonly present and correlated in HC and PFC and, as we additionally show here, in the nRE.

It is well recognized that the HC directly projects to the PFC (Swanson 1981; Ferino et al. 1987; Thierry et al. 2000; Jay and Witter 1991; Hoover and Vertes 2007). The directionality of HC-to-PFC theta synchronization has been demonstrated by recording PFC neurons firing phase locked to delayed hippocampal theta oscillations (Siapas et al. 2005). Theta synchronization is thought to play a key role in early stages of the learning, as theta coherence between these two structures increases during working memory tasks (Benchenane et al. 2010; O'Neill et al. 2013; Anderson et al. 2010; Jones and Wilson 2005; Hyman et al. 2005). For example,Benchenane et al. (2010) demonstrated in rats that coherence in theta oscillations between the HC and PFC peaked at choice points in a Y maze, and coherence was significantly greater after learning a new rule (Benchenane et al. 2010). Anderson et al. (2010) recorded from the temporal cortex and PFC in epilepsy

patients with implanted electrodes, and demonstrated increased theta coherence between HC and PFC during recall tasks that was predominately driven in the HC-to-PFC direction. In this study, we also found that theta oscillations were the dominant frequency in the HC during RPO stimulation, and that peak theta power in HC correlated to peak powers in the PFC, which agree with these earlier studies of HC-to-PFC theta synchronization.

The PFC is theorized to be a master regulator of working memory, yet the mechanism by which it influences other brain regions is not clear. The 2–5 Hz oscillation may allow for a flexible signal for the PFC to synchronize electrical activity with other brain regions. Fujisawa and Buzsaki (2011) reported a similar dominant 4-Hz (2–5 Hz band) oscillation in the PFC that was phase-coupled to HC theta and to neuronal firing in HC and the ventral tegmental area (VTA) during working memory task. As reviewed by Fujisawa and Buzsaki (2011), 2–5 Hz oscillations connecting PFC to other structures may be wide-spread, as its presence was visible in a number of previous reports even though the authors may not have emphasized them. Besides the VTA and HC, 2–5 Hz rhythm of PFC origin was present for example in striatal recordings (Dzirasa et al. 2010; Tort et al. 2008), and 2 and 4 Hz sharp narrow-band coherence with frontal cortical EEG was reported as far as in brainstem sympathetic circuits (Kenney et al. 1990). In the PFC-HC network, 4-Hz oscillation may play a complementary role with theta oscillations, such that the 4-Hz signal can phase-couple with theta by skipping every other cycle to coordinate oscillations at various frequencies across the brain (Fujisawa and Buzsaki 2011; Deshmukh et al. 2010). In our study, we found that the amplitude of theta and 4-Hz signal negatively correlated. With increasing RPO stimulation, hippocampal theta power increased, whereas prefrontal 4-Hz power decreased. This finding may be explained by bidirectional flow between the HC and PFC with one signal, either theta or 4-Hz, dominating at a given time. With increasing RPO stimulation and thus increased hippocampal theta power generation, HC-to-PFC circuit may be dominant, suppressing PFC-to-HC flow.

The role of nRE in PFC-HC coupling

Prior tracing studies demonstrate the possibility of the midline thalamic nRE as a potential candidate for mediating communication from the PFC to HC (Vertes et al. 2007; Varela et al. 2014). For theta oscillations, we found that controlling for nRE influence via partial correlations had minimal effect on HC-PFC correlation, and lidocaine inactivation also had minimal effect on HC-PFC coherence at theta. These results support prior evidence that HC-to-PFC communication occurs through a monosynaptic connection that is not be influenced by the nRE (Swanson 1981; Ferino et al. 1987; Jay and Witter 1991; Hoover and Vertes 2007). For the 4 Hz oscillation, in contrast, removal of nRE influence through partial correlations significantly affected HC-PFC correlations, and lidocaine inactivation of the nRE significantly reduced 4-Hz coherence. Together, this suggests that the nRE plays an important role in PFC-to-HC synchronization.

The inferences for understanding the dynamical network controlling PFC-HC coupling and the role of nRE, based on prior anatomy and the current findings, are summarized in Fig. 7A. Thus, theta rhythm was the dominant signal in the HC, which correlated with theta power in the PFC. This relationship was minimally affected by the nRE signal. In

comparison, the 2–5 Hz oscillation was the dominant frequency in the PFC, and correlated with the power in the HC. This signal was diminished by both statistical and pharmacologic removal of nRE influence. Although correlational analysis does not test directionality, together, these results provide strong evidence that HC-to-PFC communication occurs by synchronization of theta oscillations, whereas PFC-to-HC communication occurs through synchronization of a 4-Hz signal, and this latter is mediated by a synaptic relay in the nRE.

Two major limitations of this study should be taken into account however, i.e. that the experiments were done under urethane anesthesia, and that the data obtained are mostly correlational. Thus, further investigations are necessary both under urethane and in awake animals to understand the mechanism and function of PFC-HC coupling. Besides the core findings on the novel 2–5 Hz rhythm supported by both partial correlation and pharmacology, there are several further observations in regard of theta coupling, which although premature to fully assess at this point may stimulate further investigations. First, we found non-zero residual PFC-HC (0.13, Fig 5E) and even PFC-nRE theta (0.42, Fig. 5E) correlation when controlling for the third signal. It should be noted in this regard that besides nRE, several other structures have reciprocal connections with PFC and HC (Fig. 7A) which were not recorded in this study, but might have been the origin of these residual correlations, These include the amygdala (AMY), supramammillary nucleus (SUM), entorhinal cortex (EC), medial septum (MS), and (VTA) (McKenna and Vertes 2004; Cassel et al. 2013; Dolleman-Van der Weel et al. 1994). A monosynaptic PFC-HC projection (mainly from anterior cingulate to CA3/CA2) has also been reported recently (Rajasethupathy et al. 2015). Second, the origin and neuronal mechanisms of the PFC 2–5 Hz oscillation remains unknown. This rhythm is not necessarily generated within the PFC but may be induced by input from VTA (Fujisawa and Buzsaki 2011), from the nRE (Kiss et al. 2011a; Kiss et al. 2011d; Zhang et al. 2012; Duan et al. 2015; Nagy et al. 2016), or through a PFC-nRE reciprocal circuit (Fig. 7B). Our recordings and analysis cannot differentiate between these models; partial correlation finds unique variance between two variables which is not shared by the third variable but does not provide information on where that variance comes from. A model of a thalamo-cortical network depicted in Fig 7B could explain another interesting observation in regard of theta input i.e. controlling for PFC suppressed nRE-HC theta correlation (Fig. 5E). Third, we have only found significant PFC-HC theta correlation in half of the experiment and in these rats HC-nRE theta correlation was smaller than in the general population (cf. Figs. 4E and 5A). In fact, a greater number of rats showed theta correlations in HC-nRE and nRE-PFC pairs than PFC-HC (Fig. 4D). This might suggest that HC theta may be directed either through the HC-PFC pathway or through the nRE link toward PFC. These alternatives appeared in individual rats under urethane but may represent alternative ways of functional coupling associated with different behaviors that could be explored in future experiments in freely moving rats.

Acknowledgments

This work was supported by the National Institute of Health (Grants R01 MH100820 and P01 HL095491)

References

Anderson KL, Rajagovindan R, Ghacibeh GA, Meador KJ, Ding M. Theta oscillations mediate interaction between prefrontal cortex and medial temporal lobe in human memory. Cerebral cortex. (New York, NY : 1991). 2010; 20(7):1604–1612.

Benchenane K, Peyrache A, Khamassi M, Tierney PL, Gioanni Y, Battaglia FP, Wiener SI. Coherent theta oscillations and reorganization of spike timing in the hippocampal- prefrontal network upon learning. Neuron. 2010; 66(6):921–936. [PubMed: 20620877]

Buzsaki G. Theta oscillations in the hippocampus. Neuron. 2002; 33(3):325–340. [PubMed: 11832222]

Cassel JC, Pereira de Vasconcelos A, Loureiro M, Cholvin T, Dalrymple-Alford JC, Vertes RP. The reuniens and rhomboid nuclei: neuroanatomy, electrophysiological characteristics and behavioral implications. Progress in neurobiology. 2013; 111:34–52. [PubMed: 24025745]

Cousijn H, Tunbridge EM, Rolinski M, Wallis G, Colclough GL, Woolrich MW, Nobre AC, Harrison PJ. Modulation of hippocampal theta and hippocampal-prefrontal cortex function by a schizophrenia risk gene. Human brain mapping. 2015; 36(6):2387–2395. [PubMed: 25757652]

Deshmukh SS, Yoganarasimha D, Voicu H, Knierim JJ. Theta modulation in the medial and the lateral entorhinal cortices. Journal of neurophysiology. 2010; 104(2):994–1006. [PubMed: 20505130]

Dickerson DD, Wolff AR, Bilkey DK. Abnormal long-range neural synchrony in a maternal immune activation animal model of schizophrenia. The Journal of neuroscience : the official journal of the Society for Neuroscience. 2010; 30(37):12424–12431. [PubMed: 20844137]

Dolleman-Van der Weel MJ, Wouterlood FG, Witter MP. Multiple anterograde tracing, combining Phaseolus vulgaris leucoagglutinin with rhodamine- and biotin-conjugated dextran amine. Journal of neuroscience methods. 1994; 51(1):9–21. [PubMed: 7514701]

Duan AR, Varela C, Zhang Y, Shen Y, Xiong L, Wilson MA, Lisman J. Delta frequency optogenetic stimulation of the thalamic nucleus reuniens is sufficient to produce working memory deficits: relevance to schizophrenia. Biological psychiatry. 2015; 77(12):1098–1107. [PubMed: 25891221]

Dzirasa K, Coque L, Sidor MM, Kumar S, Dancy EA, Takahashi JS, McClung CA, Nicolelis MA. Lithium ameliorates nucleus accumbens phase-signaling dysfunction in a genetic mouse model of mania. The Journal of neuroscience : the official journal of the Society for Neuroscience. 2010; 30(48):16314–16323. [PubMed: 21123577]

Ferino F, Thierry AM, Glowinski J. Anatomical and electrophysiological evidence for a direct projection from Ammon's horn to the medial prefrontal cortex in the rat. Experimental brain research. 1987; 65(2):421–426. [PubMed: 3556468]

Fujisawa S, Buzsaki G. A 4 Hz oscillation adaptively synchronizes prefrontal, VTA, and hippocampal activities. Neuron. 2011; 72(1):153–165. [PubMed: 21982376]

Herkenham M. The connections of the nucleus reuniens thalami: evidence for a direct thalamo-hippocampal pathway in the rat. The Journal of comparative neurology. 1978; 177(4):589–610. [PubMed: 624792]

Hoover WB, Vertes RP. Anatomical analysis of afferent projections to the medial prefrontal cortex in the rat. Brain structure & function. 2007; 212(2):149–179. [PubMed: 17717690]

Hyman JM, Zilli EA, Paley AM, Hasselmo ME. Medial prefrontal cortex cells show dynamic modulation with the hippocampal theta rhythm dependent on behavior. Hippocampus. 2005; 15(6): 739–749. [PubMed: 16015622]

Ito HT, Zhang SJ, Witter MP, Moser EI, Moser MB. A prefrontal-thalamo-hippocampal circuit for goal-directed spatial navigation. Nature. 2015; 522(7554):50–55. [PubMed: 26017312]

Jay TM, Witter MP. Distribution of hippocampal CA1 and subicular efferents in the prefrontal cortex of the rat studied by means of anterograde transport of Phaseolus vulgaris-leucoagglutinin. The Journal of comparative neurology. 1991; 313(4):574–586. [PubMed: 1783682]

Jones MW, Wilson MA. Theta rhythms coordinate hippocampal-prefrontal interactions in a spatial memory task. PLoS biology. 2005; 3(12):e402. [PubMed: 16279838]

Kenney MJ, Gebber GL, Barman SM, Kocsis B. Forebrain rhythm generators influence sympathetic activity in anesthetized cats. The American journal of physiology. 1990; 259(3 Pt 2):R572–R578. [PubMed: 2396715]

Kiss T, Hoffmann WE, Hajos M. Delta oscillation and short-term plasticity in the rat medial prefrontal cortex: modelling NMDA hypofunction of schizophrenia. The international journal of neuropsychopharmacology / official scientific journal of the Collegium Internationale Neuropsychopharmacologicum (CINP). 2011a; 14(1):29–42.

Kiss T, Hoffmann WE, Scott L, Kawabe TT, Milici AJ, Nilsen EA, Hajos M. Role of Thalamic Projection in NMDA Receptor-Induced Disruption of Cortical Slow Oscillation and Short-Term Plasticity. Frontiers in psychiatry. 2011d; 2:14. [PubMed: 21556284]

Kramis R, Vanderwolf CH, Bland BH. Two types of hippocampal rhythmical slow activity in both the rabbit and the rat: relations to behavior and effects of atropine, diethyl ether, urethane, and pentobarbital. Experimental neurology. 1975; 49(1 Pt 1):58–85. [PubMed: 1183532]

Li S, Topchiy I, Kocsis B. The effect of atropine administered in the medial septum or hippocampus on high- and low-frequency theta rhythms in the hippocampus of urethane anesthetized rats. Synapse (New York, NY). 2007; 61(6):412–419.

Ly S, Pishdari B, Lok LL, Hajos M, Kocsis B. Activation of 5-HT6 receptors modulates sleep-wake activity and hippocampal theta oscillation. ACS chemical neuroscience. 2013; 4(1):191–199. [PubMed: 23336058]

McKenna JT, Vertes RP. Afferent projections to nucleus reuniens of the thalamus. The Journal of comparative neurology. 2004; 480(2):115–142. [PubMed: 15514932]

McNaughton N, Kocsis B, Hajos M. Elicited hippocampal theta rhythm: a screen for anxiolytic and procognitive drugs through changes in hippocampal function? Behavioural pharmacology. 2007; 18(5–6):329–346. [PubMed: 17762505]

McNaughton N, Sedgwick EM. Reticular stimulation and hippocampal theta rhythm in rats: effects of drugs. Neuroscience. 1978; 3(7):629–632. [PubMed: 724111]

Miller EK, Cohen JD. An integrative theory of prefrontal cortex function. Annu Rev Neurosci. 2001; 24:167–202. [PubMed: 11283309]

Nagy D, Stoiljkovic M, Menniti FS, Hajos M. Differential Effects of an NR2B NAM and Ketamine on Synaptic Potentiation and Gamma Synchrony: Relevance to Rapid-Onset Antidepressant Efficacy. Neuropsychopharmacology : official publication of the American College of Neuropsychopharmacology. 2016; 41(6):1486–1494. [PubMed: 26404843]

O'Neill PK, Gordon JA, Sigurdsson T. Theta oscillations in the medial prefrontal cortex are modulated by spatial working memory and synchronize with the hippocampus through its ventral subregion. The Journal of neuroscience : the official journal of the Society for Neuroscience. 2013; 33(35): 14211–14224. [PubMed: 23986255]

Rajasethupathy P, Sankaran S, Marshel JH, Kim CK, Ferenczi E, Lee SY, Berndt A, Ramakrishnan C, Jaffe A, Lo M, Liston C, Deisseroth K. Projections from neocortex mediate top-down control of memory retrieval. Nature. 2015; 526(7575):653–659. [PubMed: 26436451]

Sauseng P, Griesmayr B, Freunberger R, Klimesch W. Control mechanisms in working memory: a possible function of EEG theta oscillations. Neurosci Biobehav Rev. 2010; 34(7):1015–1022. [PubMed: 20006645]

Siapas AG, Lubenov EV, Wilson MA. Prefrontal phase locking to hippocampal theta oscillations. Neuron. 2005; 46(1):141–151. [PubMed: 15820700]

Sigurdsson T, Stark KL, Karayiorgou M, Gogos JA, Gordon JA. Impaired hippocampal-prefrontal synchrony in a genetic mouse model of schizophrenia. Nature. 2010; 464(7289):763–767. [PubMed: 20360742]

Swanson LW. A direct projection from Ammon's horn to prefrontal cortex in the rat. Brain research. 1981; 217(1):150–154. [PubMed: 7260612]

Thierry AM, Gioanni Y, Degenetais E, Glowinski J. Hippocampo-prefrontal cortex pathway: anatomical and electrophysiological characteristics. Hippocampus. 2000; 10(4):411–419. [PubMed: 10985280]

Tort AB, Kramer MA, Thorn C, Gibson DJ, Kubota Y, Graybiel AM, Kopell NJ. Dynamic cross-frequency couplings of local field potential oscillations in rat striatum and hippocampus during performance of a T-maze task. Proc Natl Acad Sci U S A. 2008; 105(51):20517–20522. [PubMed: 19074268]

Varela C, Kumar S, Yang JY, Wilson MA. Anatomical substrates for direct interactions between hippocampus, medial prefrontal cortex, and the thalamic nucleus reuniens. Brain structure & function. 2014; 219(3):911–929. [PubMed: 23571778]

Vertes RP. An analysis of ascending brain stem systems involved in hippocampal synchronization and desynchronization. Journal of neurophysiology. 1981; 46(5):1140–1159. [PubMed: 7299451]

Vertes RP, Hoover WB, Szigeti-Buck K, Leranth C. Nucleus reuniens of the midline thalamus: link between the medial prefrontal cortex and the hippocampus. Brain research bulletin. 2007; 71(6): 601–609. [PubMed: 17292803]

Vertes RP, Kocsis B. Brainstem-diencephalo-septohippocampal systems controlling the theta rhythm of the hippocampus. Neuroscience. 1997; 81(4):893–926. [PubMed: 9330355]

Vertes RP, Linley SB, Hoover WB. Limbic circuitry of the midline thalamus. Neuroscience and biobehavioral reviews. 2015; 54:89–107. [PubMed: 25616182]

Zhang Y, Yoshida T, Katz DB, Lisman JE. NMDAR antagonist action in thalamus imposes delta oscillations on the hippocampus. Journal of neurophysiology. 2012; 107(11):3181–3189. [PubMed: 22423006]

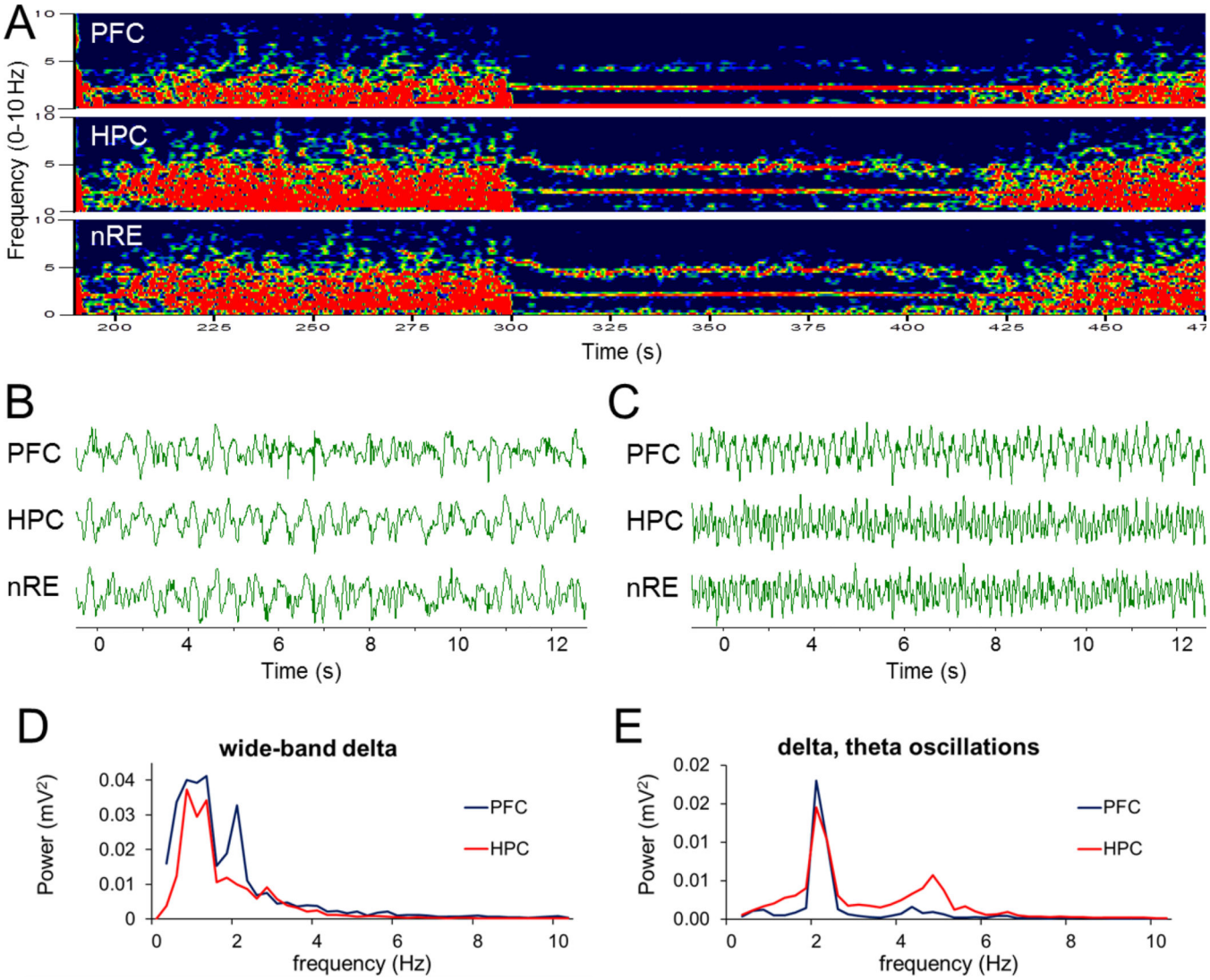

Figure 1. Spontaneous alternation between wide-band delta activity and simultaneous 2–5 Hz and theta oscillations in urethane anesthetized rats

A. Example of time-frequency plots represents alternating wide-band delta activity and two oscillations at 1.9 and 4.6 Hz in PFC, HC and nRE. B and C. Sample LFP recordings on a faster time scale showing large amplitude irregular activity (B) and rhythmic activity (C). D and E. Power spectra of 75 s PFC and HC signals exhibiting wide-band spectral components (D) and sharp peaks (E), both within the delta range (power spectra overlaid for different signals were autoscaled to the largest peak). Voltage calibration in B and C: 0.5mV.

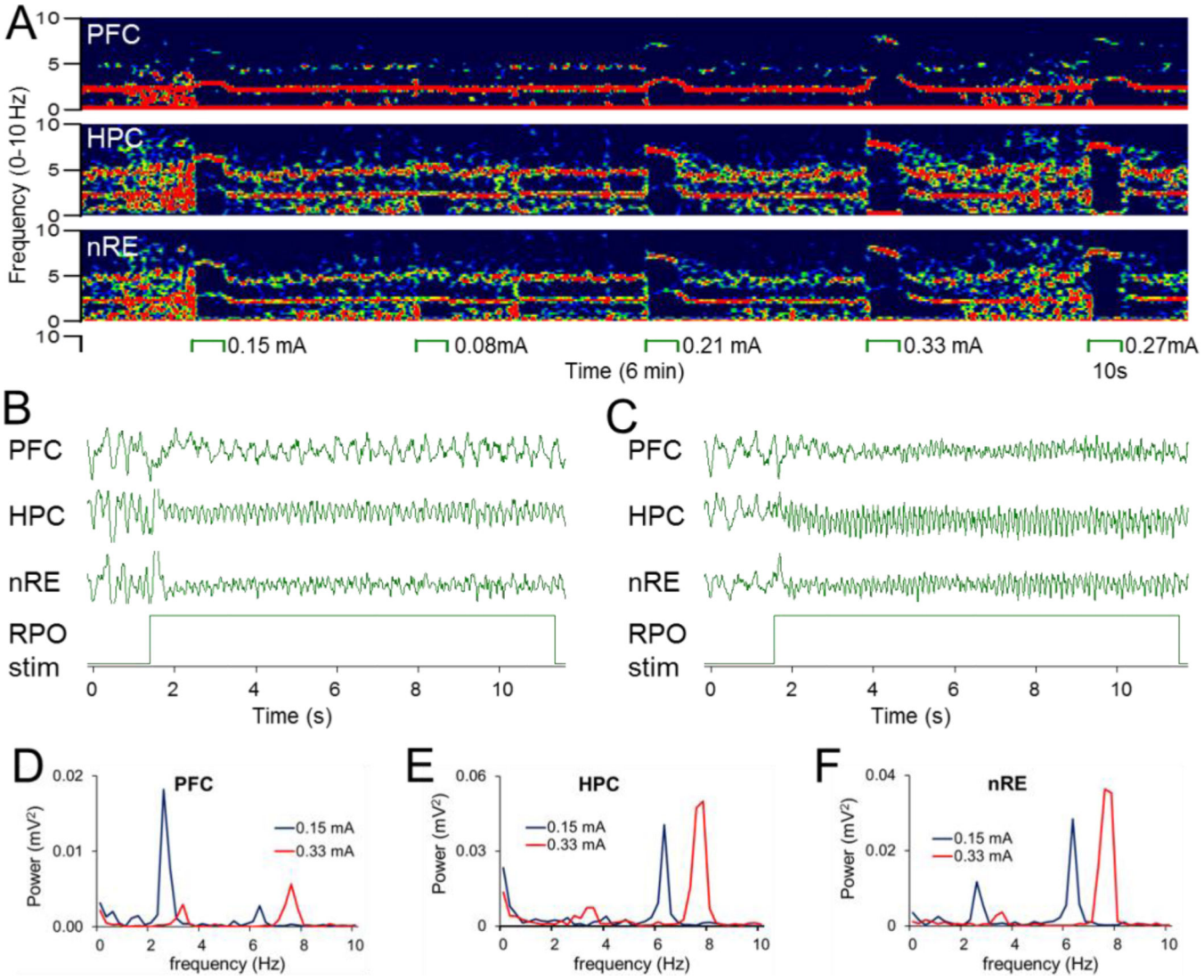

Figure 2. 2–5 Hz oscillation elicited in PFC simultaneously with HC theta by RPO stimulation

A. Time-frequency plot demonstrating PFC, HC and nRE oscillations elicited by RPO stimulation at different intensities (between 0.08 and 0.33 mA). Note 2–5 Hz and theta expressed to different extent in different signals, e.g. 2–5 Hz in PFC, theta in HC, and both in nRE at 0.15 mA, and theta only in all signals at 0.33 mA. B. Sample LFP recordings of PFC 2–5 Hz oscillation and HC theta interrupting ongoing large amplitude irregular activity at the onset of RPO stimulation at low intensity (0.15 mA). (C). High intensity (0.33 mA) RPO stimulation induced theta in all 3 signals. D–F. Power spectra of PFC (D), HC (E), and nRE (F) LFP signals shown in B and C during low (blue) and high intensity (red) RPO stimulation. Note different scales for D-F. Voltage calibration in B and C: 0.5mV.

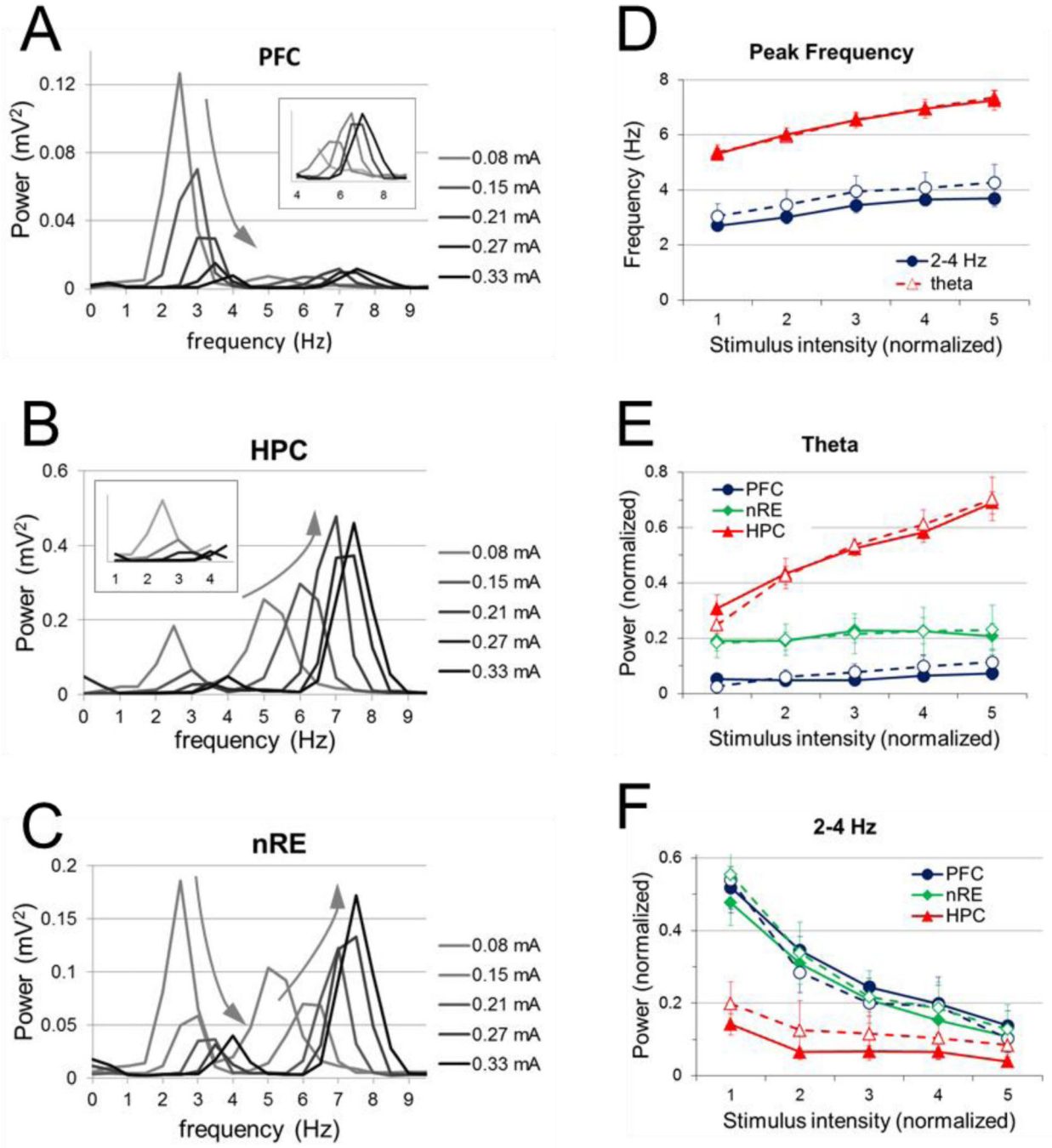

Figure 3. Changes in frequency and power of 2–5 Hz and theta oscillations elicited by stimulation of RPO at five different stimulus intensities

A–C. Sample power spectra of PFC (A), HC (B), and nRE (C) signals during RPO stimulation at different intensities. Colors represent increasing stimulus intensities. Inserts in A and B show power spectra in the frequency bands of the non-dominant components, i.e. 4–9 Hz in PFC and 1–4 Hz in HC, on a on a larger scale. Note faster and larger theta and faster and lower 2–5 Hz oscillations at higher intensities (arrows). D. Group averages of the frequency of 2–5 Hz and theta oscillations elicited by RPO stimulation at different intensities. E-F. Group averages of spectral power at theta (E) and at 2–5 Hz (F) in PFC, HC,

and nRE. Peak frequencies for theta and 2–5 Hz were identified on HC and PFC spectra, respectively, and spectral power at these frequencies, on the condition of the presence of local maxima (however small), were averaged for the three signals. In D–F, continuous lines represent averages of all rats (n=15), dashed lines represent experiments with significant PFC-HC correlation (n=7 for theta and n=13 for 2–5 Hz). Error bars represent standard error of the mean.

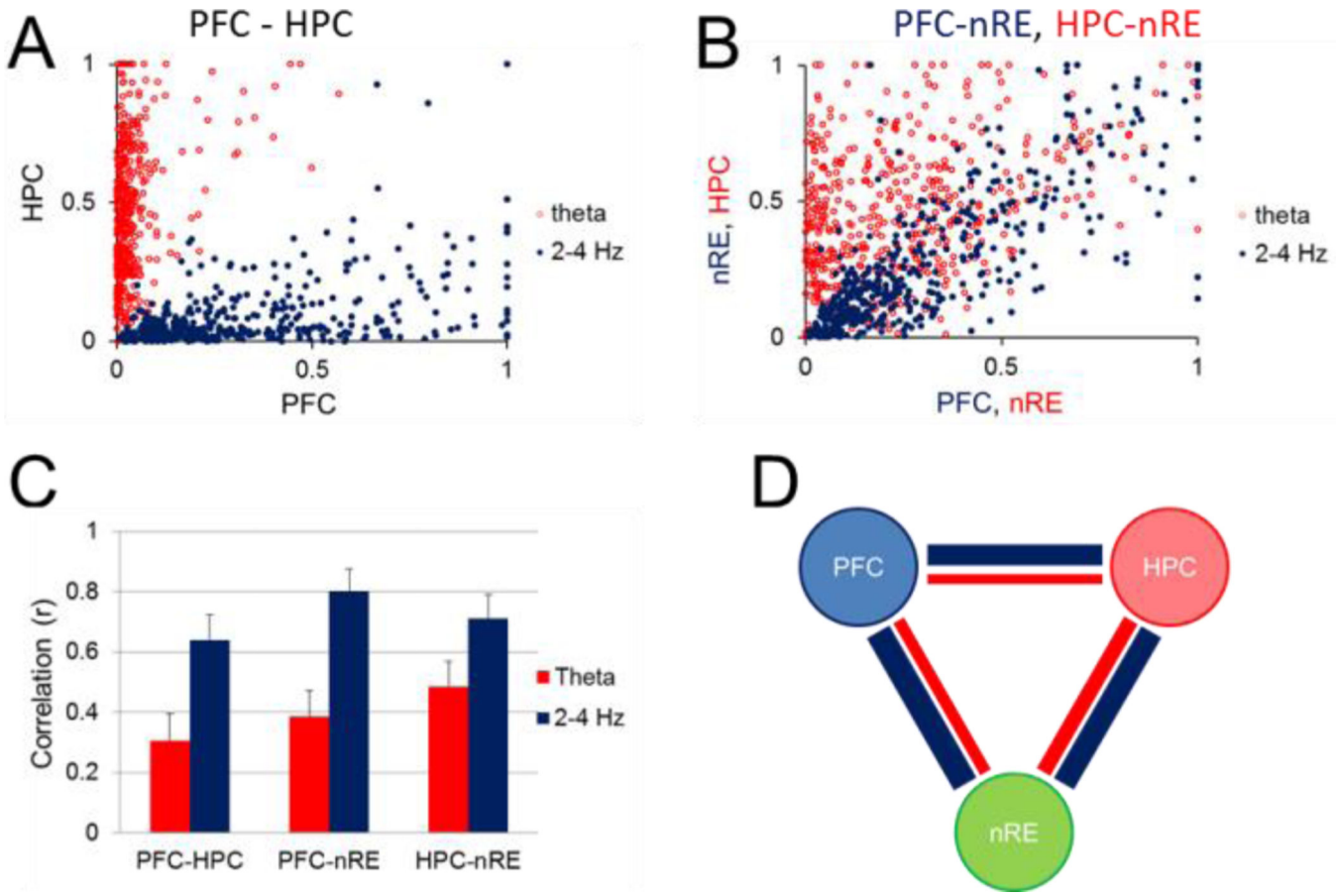

Figure 4. Relationship between PFC, HC, and nRE rhythmic LFPs at 2–5 Hz and theta frequencies

A. Scatterplot of peak power at 2–5 Hz (blue) and theta (red) frequencies in PFC and HC (all stimulation episodes, n=537 in 15 rats). B. Scatterplot of peak power in PFC vs. nRE at 2–5 Hz (blue) and HC vs. nRE at theta (red) frequencies. C. Pairwise correlation of 2–5 Hz and theta oscillations between different structures (mean±S.E.M.; correlations calculated using all data points in all rats). D. Pairwaise correlations in individual experiments (numbers show overlapping experiments with r=0). E. Pairwise correlation of 2–5 Hz and theta oscillations between different structures (mean±S.E.M.; correlations calculated separately for each rat, and averaged over the group of n=15, after non-significant correlations set to =0). F. Correlation structure of RPO induced oscillations between PFC, HC, and nRE. Thickness of lines is proportional to correlations at 2–5 Hz (blue) and theta (red) frequencies. In A and B, LFP voltages were normalized for each experiment and expressed in arbitrary units (between 0 and 1).

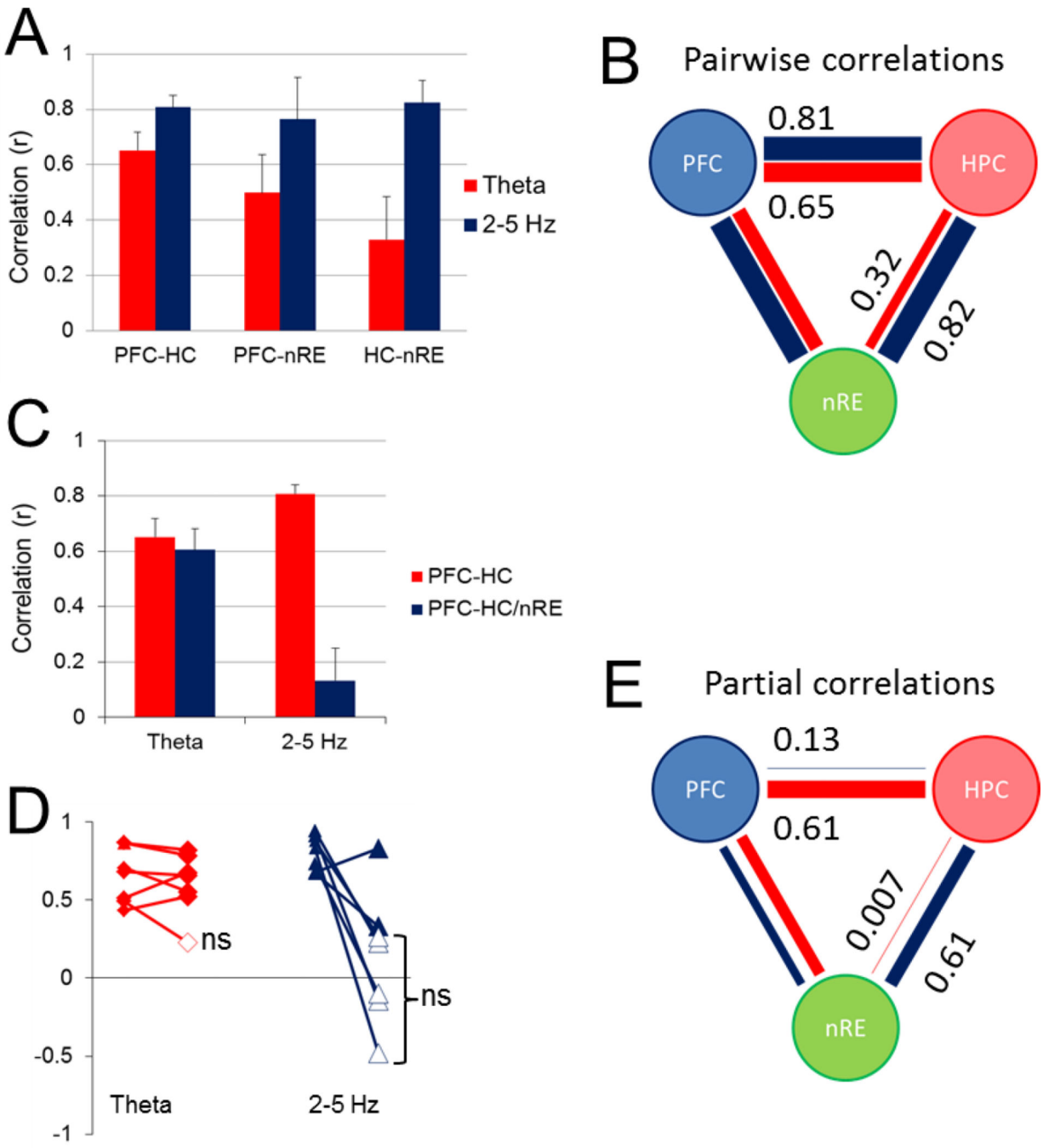

Figure 5. Partialization of significant PFC-HC correlations by nRE

A. Group averages of pairwise correlation of 2–5 Hz and theta oscillations between PFC, HC, and nRE, only including experiments with significant PFC-HC correlations at both frequencies (n=7). B. Correlation structure of RPO induced oscillations between PFC, HC, and nRE for this group. C and D. PFC-HC correlations and PFC-HC/nRE partial correlation: group averages (C), and the effect of partialization in individual experiments (ns: partial correlation not significantly different from zero) (D). E. Pairwise partial correlations after controlling for the third signal. Note complete elimination of PFC-HC 2–5 Hz correlation

and HC-nRE theta correlation. Note also relatively high and equal residual PFC-nRE correlations at the 2 frequencies (theta: 0.42; 2–5 Hz: 0.44). In B and E thickness of lines is proportional to peak correlations at 2–5 Hz (blue) and theta (red) frequencies.

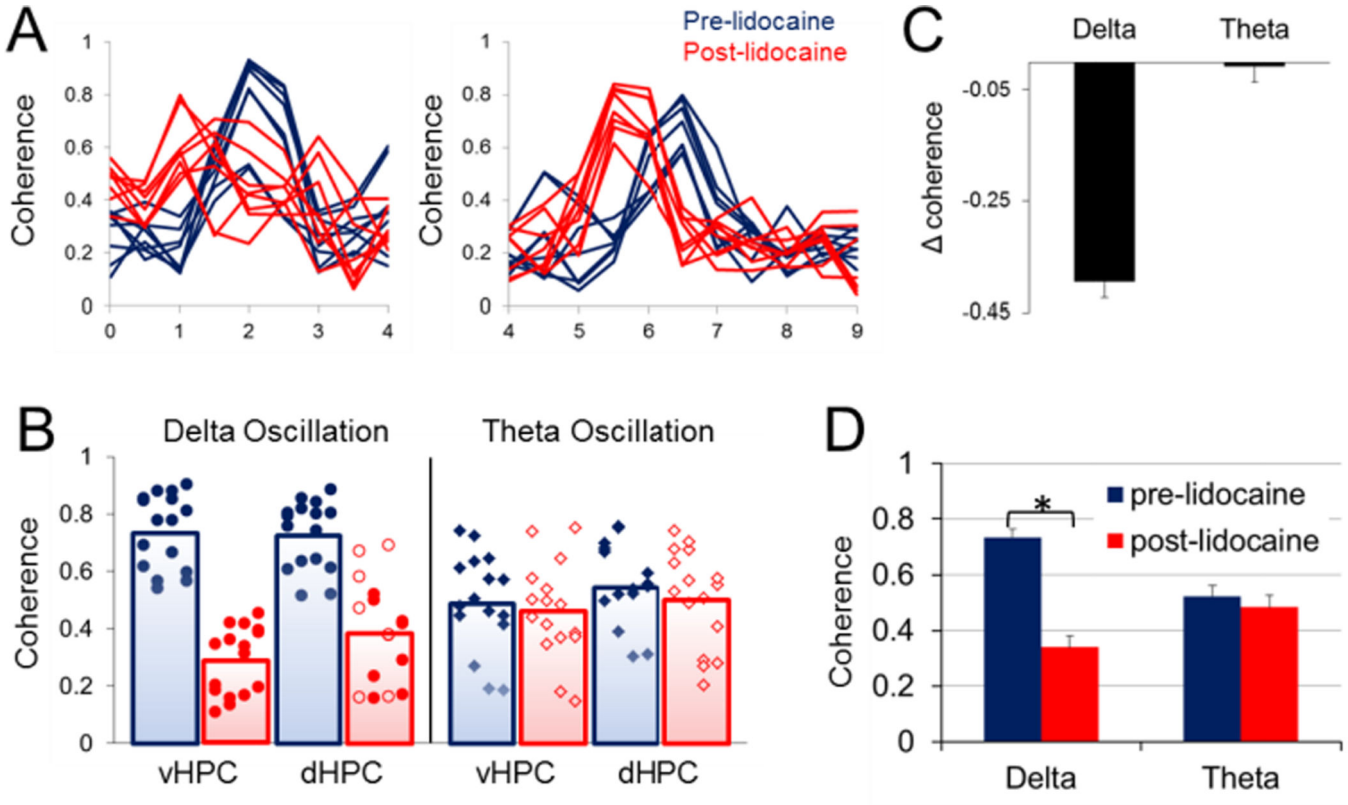

Figure 6. Effect of nRE inactivation on HC-PFC delta and theta coherence

A. Coherence spectra of all pairwise combinations between 2 PFC and 4 HC recordings in the delta (0–4 Hz, left) and theta (4–9 Hz) frequency ranges before (blue) and after (red) microinjection of 0.1 mg (1 uL, 0.374 uL/min) lidocaine in the nRE. Sample coherence spectra from a representative experiment are shown during low (left) and high (right) RPO stimulation. B. Pre- and post-lidocaine peak coherence for pairs of PFC-vHC and PFC-dHC recordings. Individual peaks are plotted as dots (delta) or rhomboids (theta); open symbols mark experiments with no significant drug effect. Each bar represents the mean of peak coherence values in one condition, for all rats. C. The change in peak delta and theta coherence after lidocaine injection, averaged over all PFC-HC pairs (n= 32 combinations in 4 rats). D. Group averages of coherence peak values in pre- and post-lidocaine recordings. Pharmacological inactivation of the nRE had minimal effect on coherence between the PFC and HC for theta oscillations ($p = 0.19$), whereas significant decreased the coherence for oscillation in the delta range ($p < 0.001$).

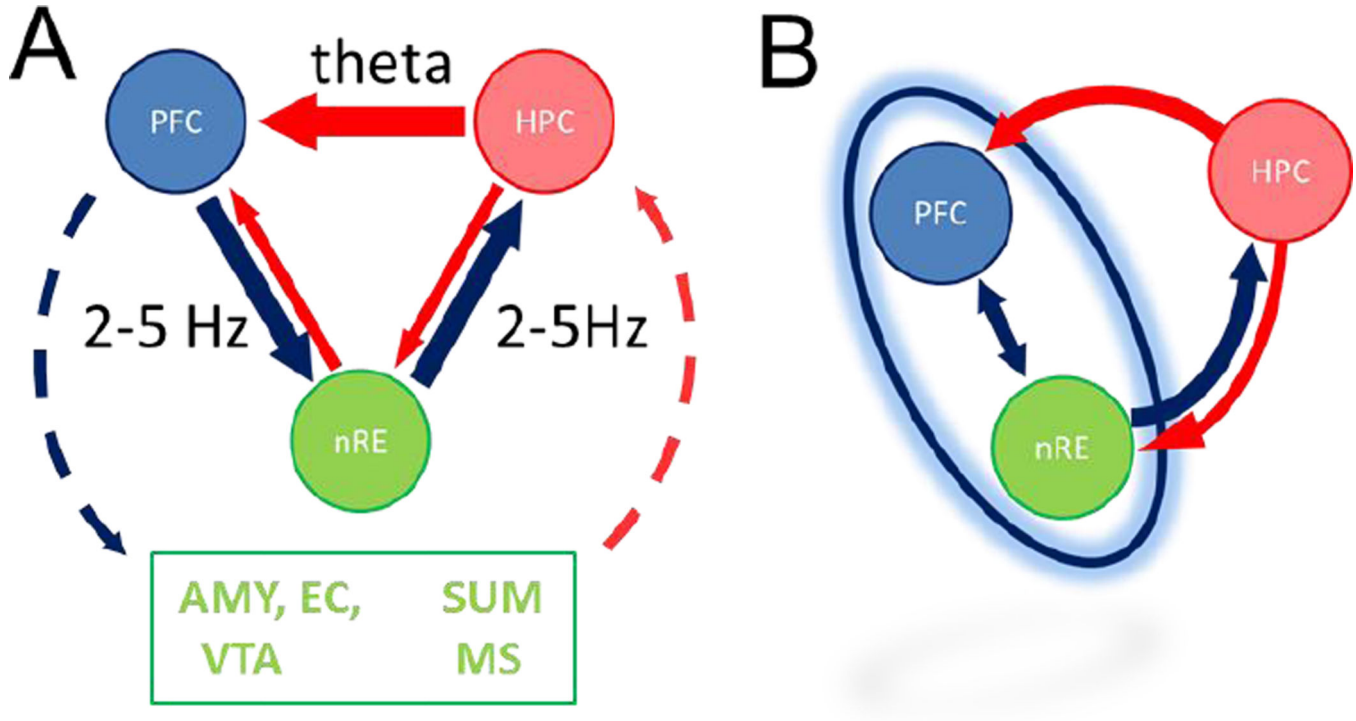

Figure 7. Possible models of HC-PFC oscillatory coupling at two frequencies

A. Model summarizing the known anatomical connections and their selective involvement, as shown in this study, in conveying 2–5 Hz and theta oscillatory signal between PFC and HC. First, our data are in agreement with the direct HC-to-PFC pathway carrying theta synchronizing signal. Second, synchronization at 2–5 Hz was found to involve the nRE and could use reciprocal nRE connections with both PFC and HC. Third, several other structures, not recorded in this study, also have reciprocal connections with PFC and HC and could be the origin of residual correlations, including the amygdala (AMY), supramammillary nucleus (SUM), entorhinal cortex (EC), medial septum (MS), and ventral tegmental area (VTA). B. Functional model in which the 2–5 Hz oscillation is generated by a thalamo-cortical (nRE-PFC) network. The primary input to this network receiving HC theta influence is the PFC. A secondary input for HC theta directed to this network is available through the nRE. The common output of the network through which 2–5 Hz synchronizing signal can be sent to the HC is the nRE.